Am J Nucl Med Mol Imaging 2024;14(2):110-121
www.ajnmmi.us /ISSN:2160-8407/ajnmmi0154190

Original Article

^{68}Ga-labeled TMTP1 radiotracer for PET imaging of cervical cancer

Xi Chen[1,2,5*], Yue Sun[1,2*], Fei Li[1,2], Ling Xi[1,2], Jun Dai[1,2], Can Zhao[4#], Qingjian Dong[3#]

[1]Department of Obstetrics and Gynecology, Tongji Hospital, Tongji Medical College, Huazhong University of Science and Technology, Wuhan 430030, Hubei, China; [2]National Clinical Research Centre for Obstetrics and Gynaecology, Cancer Biology Research Centre (Key Laboratory of The Ministry of Education), Tongji Hospital, Tongji Medical College, Huazhong University of Science and Technology, Wuhan 430030, Hubei, China; [3]Department of Nuclear Medicine, Tongji Hospital, Tongji Medical College, Huazhong University of Science and Technology, Wuhan 430030, Hubei, China; [4]Department of Pathology, Tongji Hospital, Tongji Medical College, Huazhong University of Science and Technology, Wuhan 430030, Hubei, China; [5]Department of Obstetrics and Gynecology, The First Affiliated Hospital of Zhengzhou University, Zhengzhou 450052, Henan, China. [*]Equal contributors. [#]Equal contributors.

Received October 31, 2023; Accepted April 2, 2024; Epub April 25, 2024; Published April 30, 2024

Abstract: Molecular imaging enables visualization and characterization of biological processes that influence tumor behavior and response to therapy. The TMTP1 (NVVRQ) peptide has shown remarkable affinity to highly metastatic tumors and and its potential receptor is aminopeptidase P2. In this study, we have designed and synthesized a ^{68}Ga-labeled cyclic TMTP1 radiotracer (^{68}Ga-DOTA-TMTP1), for PET imaging of cervical cancer. The goal of this study was to investigate the properties of this radiotracer and its tumor diagnostic potential. The radiochemical yield of ^{68}Ga-DOTA-TMTP1 was high and the radiochemical purity was greater than 95%. The octanol-water partition coefficient for ^{68}Ga-DOTA-TMTP1 was -2.76 ± 0.08 and ^{68}Ga-DOTA-TMTP1 has showed excellent stability in in vitro studies. The cellular uptake and efflux of ^{68}Ga-DOTA-TMTP1 in paired highly metastatic and lowly metastatic cervical cancer cell line HeLa and C-33A as well as normal cervical epithelial cell line End1 were measured in a γ counter. ^{68}Ga-DOTA-TMTP1 exhibited higher uptake in HeLa cells than in C-33A cells. The binding to HeLa and C-33A cells could be blocked by excess TMTP1. On microPET images, HeLa tumors were clearly visualized within 60 min and the uptake of the radiotracer in HeLa tumors was higher than that of C-33A tumors. After blocking with TMTP1, HeLa tumors uptake was significantly reduced and the specificity ^{68}Ga-DOTA-TMTP1 was thus validated. Overall, we have successfully synthesized ^{68}Ga-DOTA-TMTP1 with high yield and high specific activity and have demonstrated its potential role for highly metastatic tumor-targeted diagnosis.

Keywords: Cervical cancer, ^{68}Ga-DOTA-TMTP1, positron emission tomography, molecular imaging, metastasis

Introduction

Cervical cancer is a common malignant tumor of the female reproductive tract, which seriously endangers women's lives and health [1, 2]. The prognosis of cervical malignancy is affected by stage of the diseases, histological grading of tumor, the occurrence of HPV infection, etc. [3]. Although staging of cervical cancer plays a vital role in patient management, the current FIGO staging system is predominantly based on clinical examinations which provides limited ability to accurately comprehend the disease status, including failure in providing nodal involvement and the extent of metastasis [4]. Imaging studies are recommended for cervical cancer work up [3, 5]. However, traditional imaging techniques have largely relied on anatomical changes and size criteria for lesion detection and exhibit poor sensitivity towards minor lesions. Therefore, developing novel molecular imaging agents with high sensitivity and tumor-targeting ability may somehow assist in accurate staging and provide more appropriate interventions [6].

Previously our group had identified a novel five-amino acid peptide, TMTP1 (Asn-Val-Val-Arg-Gln, NVVRQ), by FliTrx bacterial peptide display system [7]. TMTP1 is a tumor-homing peptide which specifically targets highly metastatic tumors and metastasis and its potential receptor is aminopeptidase P (XPNPEP2). XPNPEP2 is overexpressed in cervical cancer, and was associated with the International Federation of Gynecology and Obstetrics stage and lymph node metastasis [8]. In our previous studies, TMTP1-based agents have shown potential for tumor-targeting diagnosis and therapy. Our group has developed various TMTP1-based fusion proteins which can target highly metastatic tumors and produce oncotoxic effects [9-14]. For example, we have fused TMTP1 to the NF-κB essential modulator-binding domain and the trans-activator of transcription peptide, the resulting peptide TMTP1-TAT-NBD enhanced anticancer effects by downregulating AKT/GSK-3β/NF-κB pathway [9]. TMTP1-DKK, which is a combination of an antimicrobial peptide, D(KLAKLAK)^2, with TMTP1, causes apoptosis in human prostate and gastric cancer cells [10]. With respect to tumor-targeted imaging, we have reported a ^{99m}Tc-labeled TMTP1 radiotracer for SPECT imaging and demonstrated its ability to target highly metastatic ovarian tumors [12]. Yesen et al. synthesized an ^{18}F-labeled TMTP1 tracer aimed at highly aggressive hepatocellular carcinoma imaging [14].

However, SPECT-based tracers have limited resolution and sensitivity for tumor imaging and ^{18}F-labeling depends

https://doi.org/10.62347/NFDH6303

on the availability of a cyclotron and is time-consuming and laborious [15, 16]. ^{68}Ga ($t_{1/2}$ 68 min, β^+ emission, 89% and EC 11%) is an ideal radionuclide for imaging because of its short half-life, low radiation dosimetry, rapid blood clearance, quick fusion and targeted localization [17]. The hydrophilicity and short half-life of ^{68}Ga makes it suitable for labeling small molecular weight binding proteins or peptides with fast distribution and renal clearance [18, 19]. To the best of our knowledge, application of TMTP1-based tracers labeled with ^{68}Ga for cervical cancer screening have not yet been reported.

Our study entails the design and synthesis of a novel ^{68}Ga-labeled PET tracer for tumor imaging and diagnosis. This present work conjugates cyclic TMTP1 [cyclo(CGNVVRQGC)] with 1,4,7,10-tetraaza-cyclododecane-1,4,7,10-tetraacetic acid (DOTA) as chelator and triglycine (G_3 = Gly-Gly-Gly) acts as a spacer linking the chelate to the peptides. The resulting agent [^{68}Ga]Ga-DOTA-Gly_3-TMTP1 (^{68}Ga-DOTA-TMTP1) was thoroughly investigated in preliminary studies of cervical cancer xenografts. For new FIGO staging of cervical cancer, MRI with high spatial resolution is expected for tumour size measurements and the high accuracy of positron emmision tomography/CT for LN evaluation [20]. The sensitivity of PET-CT in diagnosing cervical cancer lymph node metastasis is only 50% for abdominal lymph nodes and 83% for pelvic lymph nodes, and more accurate imaging diagnosis has been required [21].

Materials and methods

General

All starting reagents which were purchased from commercial sources were of analytical grade and were used without further purification. The radiochemical precursor DOTA-TMTP1 (DOTA-GGG-cyclo(CGNVVRQGC)) was synthesized by Abgent Biotechnology (Suzhou, China) using solid-phase Fmoc chemistry. The chemical purity of the precursor was analyzed by high performance liquid chromatography (HPLC) and the compound was evaluated by liquid chromatography-mass spectrometry (LC-MS). ^{68}Ga was eluted from a ^{68}Ge/^{68}Ga generator (Isotope Technologies Garching GmbH, Germany) by 5 ml of 0.1 *N* HCl. Reverse-phase extraction Sep-Pak C18 cartridges were purchased from Waters Corporation (Milford, USA) and were pretreated with ethanol (10 ml) and pure water (10 ml) before use. Radioactivity was measured by a CRC-25R Dose Calibrator (Capintec, Inc., USA). Radiochemical purity and in vitro stability was performed by instant thin-layer chromatography silica gel (ITLC-SG) analysis.

Radiosynthesis

^{68}Ga-labeling was performed in accordance with the manufacturer's protocol. In brief, 93 µl of 1.25 M NaOAc buffer was mixed with 1 ml of $^{68}GaCl_3$ eluent and the solution was adjusted to pH 4.0. Then 20 µg of DOTA-TMTP1 peptide was dissolved in the buffer for 15 min at 100°C. The product was then purified with Sep-Pak C18 cartridges and eluted with 0.5 ml of 75% ethanol. The mixture was diluted by saline and passed through a 0.22-µm Millipore filter into a sterile vial for in vitro and in vivo experiments. The product purity was evaluated by ITLC-SG with the mobile phase of CH_3OH:NH_4OAc (v/v, 1:1).

Octanol-water partition coefficient

500 µL of ^{68}Ga-labeled DOTA-TMTP1 (370 Kbq, 10 µCi) diluted in saline was added to 500 µL of n-octanol in a 1.5 mL Eppendorf microcentrifuge tube. The mixture was vortexed for 2 min at room temperature and then centrifuged at 3000 rpm for 5 min. 100 µL aliquots were sampled from each layer and were measured by a γ-counter. The experiment was performed in triplicates and the log *P* value (log_{10} (counts in n-octanol/counts in saline)) was expressed as mean ± SD.

Stability evaluation in vitro

^{68}Ga-DOTA-TMTP1 (500 µL, about 18.5 MBq) was dissolved in 1 ml aliquots of saline or human serum from healthy donors and incubated at 37°C. At 15, 30, 60 and 120 minutes, the radiochemical purity was measured by ITLC-SG using the mobile phase of CH_3OH:NH_4OAc (v/v, 1:1).

Cell lines and cervical cancer xenograft models

The human cervical epithelial cell line End1 and the human cervical cancer cell lines C-33A and Hela were obtained from the American Type Culture Collection (ATCC, Manassas, VA, USA). End1 cells were maintained in keratinocyte serum-free medium supplemented with 0.05 mg/mL bovine pituitary extract, 0.1 ng/mL human recombinant epithelial growth factor, and 44.1 mg/L calcium chloride. C-33A, Hela were cultured in DMEM supplemented with 10% fetal bovine serum (FBS). All the cells were cultured in a humidified incubator with 5% CO_2 at 37°C. All animal experiments were approved by the Institutional Animal Care and Use Committee of Peking Union Medical College hospital, and the study was conducted in strict accordance with the Guidelines for the Welfare of Animals in Experimental Neoplasia. For the xenograft tumor studies, we purchased four-week-old female BALB/c-null mice from Beijing HFK Bio-technology Co., Ltd. Hela and C-33A tumor-bearing models were established by subcutaneous injection of 1×10^7 cells in BALB/c-null mice. At approximately 3-4 weeks after inoculation, the tumor volume reached 100-300 mm^3 and the mice underwent PET imaging and biodistribution studies.

Cell migration and invasion assays

Cell migration was assessed by the wound healing assay. Human cervical cancer cells were seeded in six-well plates until 80% confluence. A sterile 10 µL pipette tip

was used to generate the wound. Images were captured at 24 h and the area was assessed by Image J software. For invasion assays, transwell inserts with 8-μm pores were precoated with 50 μL of matrigel matrix. The cells were seeded into the upper chamber at a density of 1×10^4 cells/well with 100 μL serum-free DMEM medium. DMEM medium with 10% FBS acted as a chemoattractant in the lower chamber. After 24 h of incubation, the cells which had invaded through the millipores were stained with 0.5% crystal violet. The number of invading cells were photographed and counted under a microscope. All experiments were performed in triplicate wells and at least three times.

Cell uptake and efflux studies

The cell uptake and efflux assays were inspired from previous literature methodologies and modified accordingly [19, 20]. For uptake studies, the End1, C-33A and Hela cells were seeded into the 24-well plates at a density of 1×10^5 cells per well and incubated with ^{68}Ga-DOTA-TMTP1 (about 18.5 KBq/well) at 37°C for 15, 30, 60, 120 min. The cells were then washed three times with ice-cold PBS to remove the unbounded radioactivity and digested with 0.25% trypsin. The cell suspensions in each well were collected and the internalized radioactivity was measured in a γ-counter (Packard, Meriden, CT).

Blocking study was performed in Hela and C-33A cells to assess the specificity of ^{68}Ga-DOTA-TMTP1. The cells were pretreated with 10 μg of cold TMTP1 for 15 min and then incubated for 1 h and 2 h with the radiotracer. The cell suspensions were processed and measured in the same way as formerly described.

For efflux studies, End1, C-33A and Hela cells cultured in 24-well plates were first incubated with ^{68}Ga-DOTA-TMTP1 (about 18.5 KBq/well) at 37°C for 1 h to allow maximal internalization. Then, the cells were washed three times with PBS to remove the unbounded radioactivity and incubated with prewarmed culture medium for 15, 30, 60, 120 min at 37°C. Subsequently, the cells were washed three times with PBS and digested by trypsinization with 0.25% trypsin. The resulting solution from each well was collected and measured in a γ counter. Data is expressed as the percentage of added dose after decay correction. The same experiment was performed twice with triplicate wells.

MicroPET imaging

The imaging study was performed using the Hela and C-33A tumor-bearing mice. Each mouse was administered intravenously with ^{68}Ga-DOTA-TMTP1 (about 200 μCi) via tail vein under isoflurane anesthesia (n = 3 per group). Imaging was performed with a small-animal PET scanner (BioCaliburn LH Raycan Technology Co., Ltd., Suzhou, China). Static images were acquired at different time points (5 min, 30 min, 60 min) postinjection. 60 min-dynamic scans were performed using BALB/C-null mice (6×10 s, 9×60 s, 4×5 min, 3×10 min, total of 22 frames). Images were reconstructed using a three-dimensional ordered subsets expectation maximum algorithm without attenuation correction. For the blocking study, Hela-tumor bearing mice were co-injected with excess TMTP1 at 15 mg/kg body weight and 200 μCi ^{68}Ga-DOTA-TMTP1 and the PET scans were then performed at 30 min after injection (n = 3 per group). Regions of interests (ROIs) were drawn over the tumor and major organs and tissues using Amide data analysis software.

Biodistribution studies

Female athymic nude mice bearing Hela xenografts were injected with 100 μCi of ^{68}Ga-DOTA-TMTP1 to evaluate the distribution of the tracer in the tumor and major organs and tissues. At 10, 30, and 60 min after injection of the tracer, the animals were euthanized and dissected. Tumor, blood, major organs and tissues were collected and weighted. The radioactivity was measured using a γ counter. The counts were converted into the percentage of injected dose per gram of tissue (%ID/g). Values are expressed as mean ± SD for groups of three mice.

Statistical analysis

All the quantitative results are presented as means ± SD. Statistical analyses were performed with Prism 6.0 GraphPad software. Student's t-test was used to make comparisons between two groups. A p-value < 0.05 was considered significant.

Results

Synthesis and radiolabeling of DOTA-TMTP1

The precursor DOTA-TMTP1 was synthesized with a purity of 95.495% based on HPLC analysis and the identity of the product was confirmed by LC-MS (Supplementary Figure 1A-C). The scheme for radiolabeling of DOTA-TMTP1 is presented in **Figure 1A**. Fresh ^{68}Ga eluted from the ^{68}Ge/^{68}Ga generator was used directly for the reaction under pH 4.0. The labeling process took about 30 min, with a radiochemical yield of 87.87 ± 5.90% and radiochemical purity of greater than 95% was reached after purification by Sep-Pak C18 cartridges which was characterized by ITLC analysis (**Figure 1B**). The molar activity of purified ^{68}Ga-DOTA-TMTP1 was determined to be about 16.54 MBq/*n*mol and the log *P* value of ^{68}Ga-DOTA-TMTP1 was -2.76 ± 0.08.

In vitro stability

^{68}Ga-DOTA-TMTP1 displayed good stability in saline and human serum. After incubation in saline and human serum, the samples were analyzed by ITLC at different time points. The radiochemical purity of the product

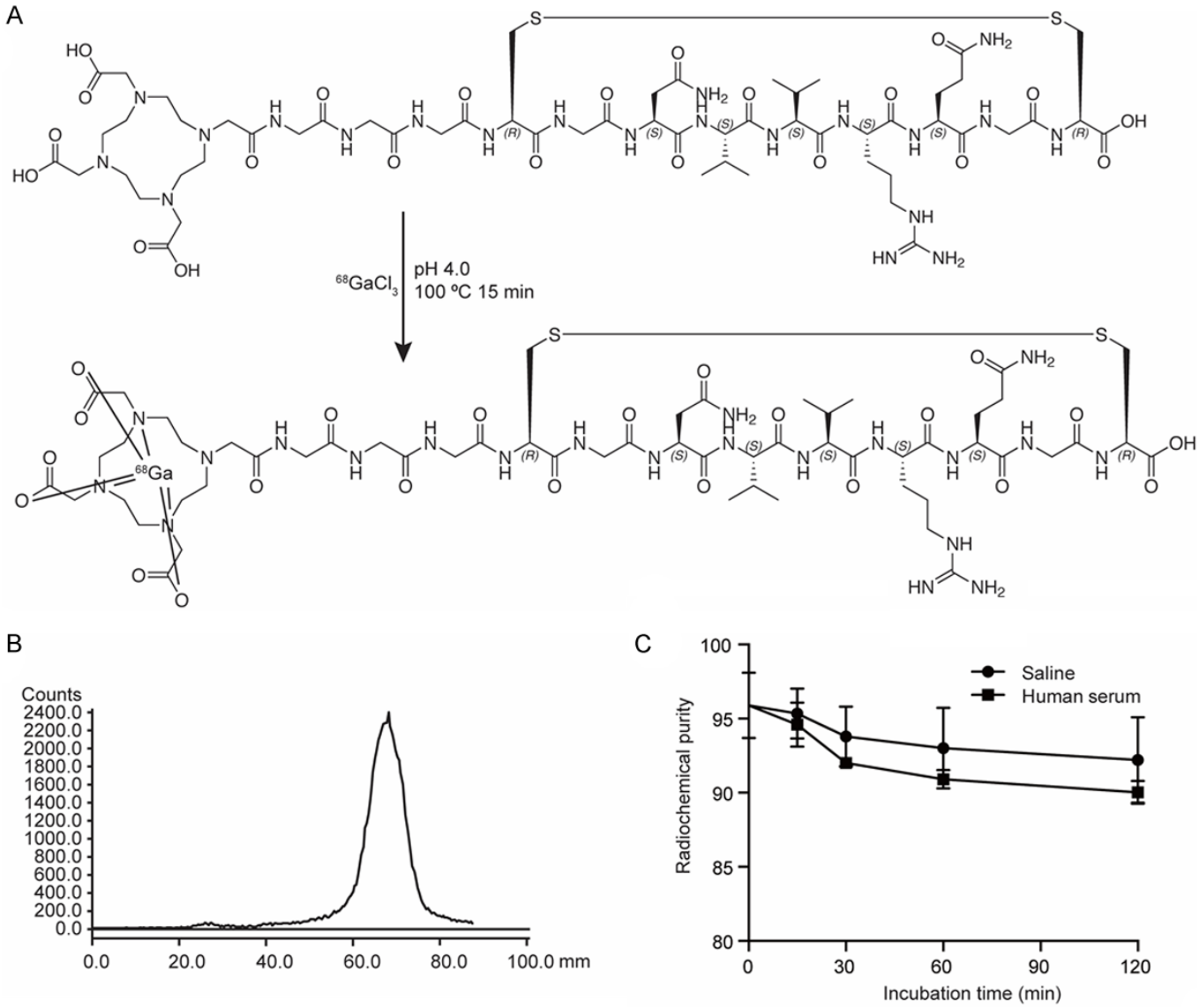

Figure 1. Radiosynthesis, purification and stability of ^{68}Ga-DOTA-TMTP1. A. Chemical structure and radiosynthesis of ^{68}Ga-DOTA-TMTP1. B. Representative ITLC assay of ^{68}Ga-DOTA-TMTP1 after purification through Sep-Pak C18 cartridges. C. In vitro stability analysis of ^{68}Ga-DOTA-TMTP1 in saline and fresh human serum at 15, 30, 60, 120 min. Results are plotted as the radiochemical purity.

remained more than 86% after 2 h incubation at 37°C (**Figure 1C**). Overall, ^{68}Ga-DOTA-TMTP1 demonstrated favorable in vitro stability.

Cell uptake and efflux studies

Cell migration and invasion ability of Hela was significantly higher than that of C-33A (**Figure 2A-D**). The cell uptake and efflux of ^{68}Ga-DOTA-TMTP1 were evaluated in the paired highly metastatic and lowly metastatic cervical cancer cell line Hela and C-33A as well as in normal cervical epithelial cell line End1 (**Figure 2E**, **2F**). Hela had rather rapid and high uptake of ^{68}Ga-DOTA-TMTP1 and End1 had relatively low uptake of the tracer. The uptake curve of C-33A was between those of Hela and End1 cells. The cellular retention of ^{68}Ga-DOTA-TMTP1 also followed the order Hela > C-33A > End1. Hela, C-33A and End1 retention of the tracer decreased with time. At 120 min, the cell-bound tracers were 2.40 ± 0.11% for Hela, 0.74 ± 0.10% for C-33A and 0.02 ± 0.02% for End1, respectively. An excess of cold TMTP1 acted as the blocking agent. For both Hela and C-33A cells, the uptake of ^{68}Ga-DOTA-TMTP1 was significantly reduced in the blocking groups when compared with non-blocking groups (**Figure 2G**, **2H**). For Hela cells, the uptake of ^{68}Ga-DOTA-TMTP1 was 2.73 ± 0.18% (non-block) and 1.01 ± 0.19% (block, $P < 0.001$) at 1 h, and 3.14 ± 0.25% (non-block) and 1.39 ± 0.15% (block, $P < 0.001$) at 2 h (**Figure 2G**). For C-33A cells, the uptake of ^{68}Ga-DOTA-TMTP1 was 1.08 ± 0.16% (non-block) and 0.37 ± 0.13% (block, $P < 0.01$) at 1 h, and 1.41 ± 0.14% (non-block) and 0.55 ± 0.07% (block, $P < 0.001$) at 2 h (**Figure 2H**).

MiroPET imaging

A series of dynamic ^{68}Ga-DOTA-TMTP1 PET images are presented in **Figure 3**. The tracer shows fast clearance from the urinary system. ^{68}Ga-DOTA-TMTP1 rapidly

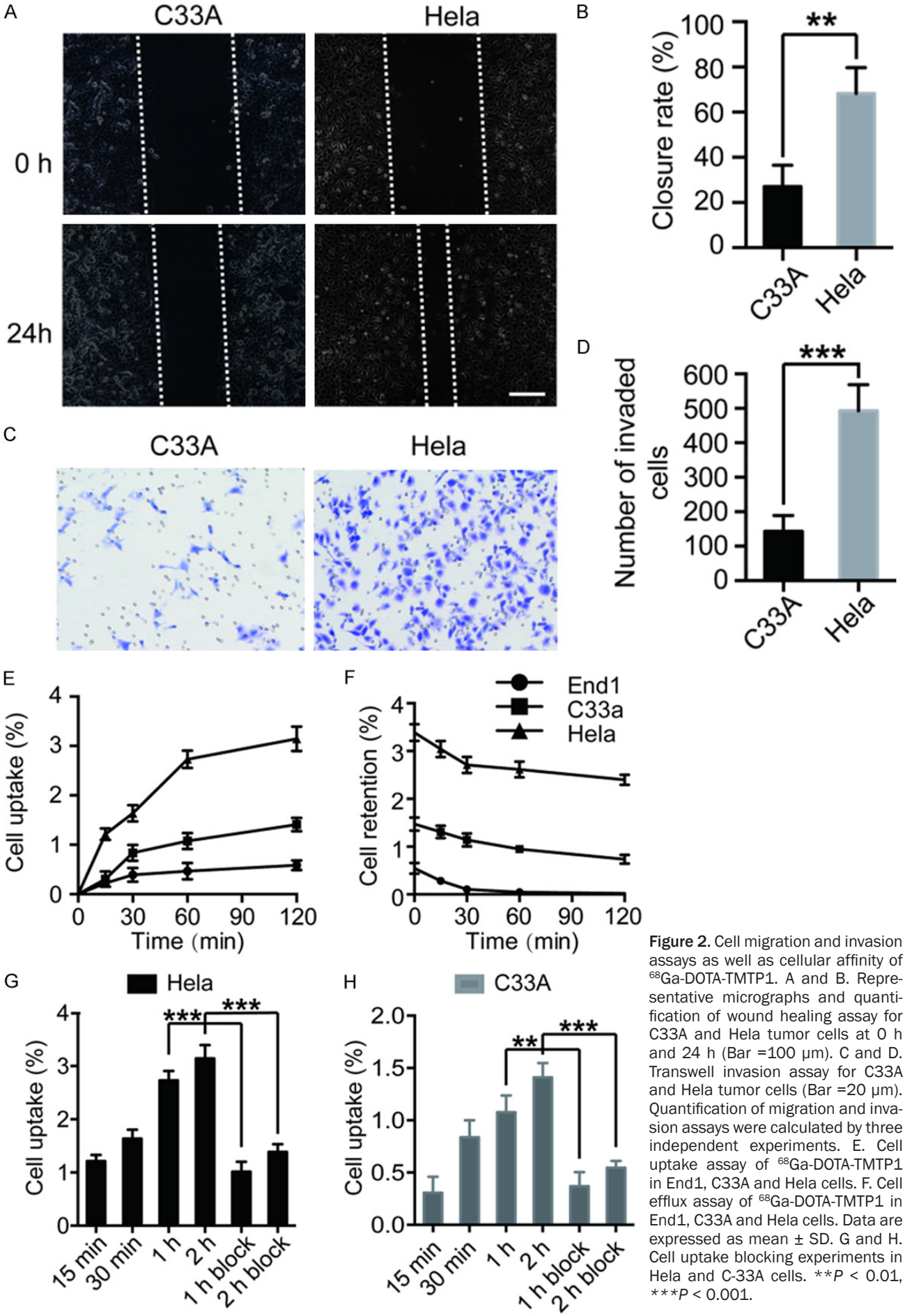

Figure 2. Cell migration and invasion assays as well as cellular affinity of ^{68}Ga-DOTA-TMTP1. A and B. Representative micrographs and quantification of wound healing assay for C33A and Hela tumor cells at 0 h and 24 h (Bar =100 μm). C and D. Transwell invasion assay for C33A and Hela tumor cells (Bar =20 μm). Quantification of migration and invasion assays were calculated by three independent experiments. E. Cell uptake assay of ^{68}Ga-DOTA-TMTP1 in End1, C33A and Hela cells. F. Cell efflux assay of ^{68}Ga-DOTA-TMTP1 in End1, C33A and Hela cells. Data are expressed as mean ± SD. G and H. Cell uptake blocking experiments in Hela and C-33A cells. $^{**}P < 0.01$, $^{***}P < 0.001$.

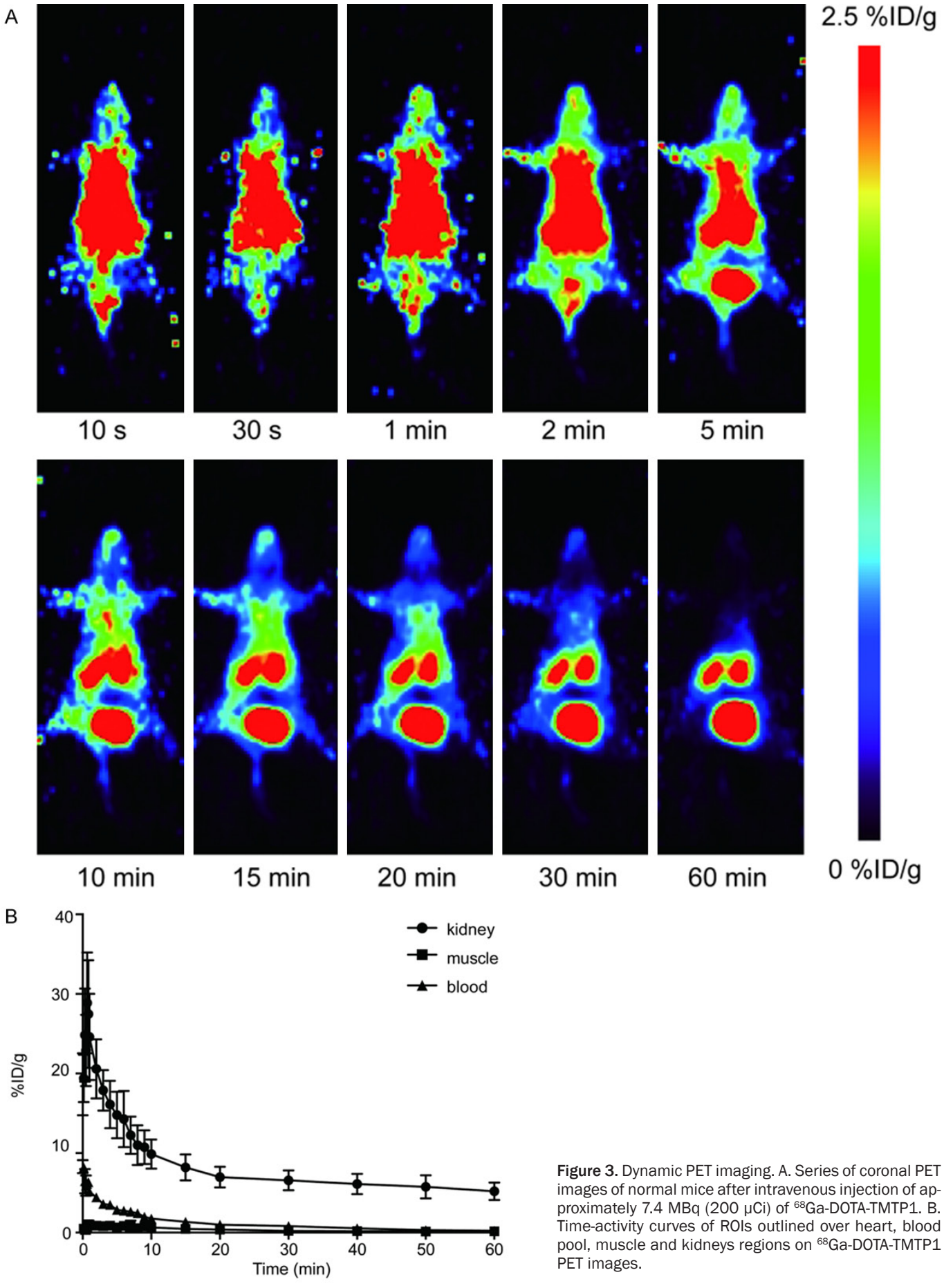

Figure 3. Dynamic PET imaging. A. Series of coronal PET images of normal mice after intravenous injection of approximately 7.4 MBq (200 μCi) of [68]Ga-DOTA-TMTP1. B. Time-activity curves of ROIs outlined over heart, blood pool, muscle and kidneys regions on [68]Ga-DOTA-TMTP1 PET images.

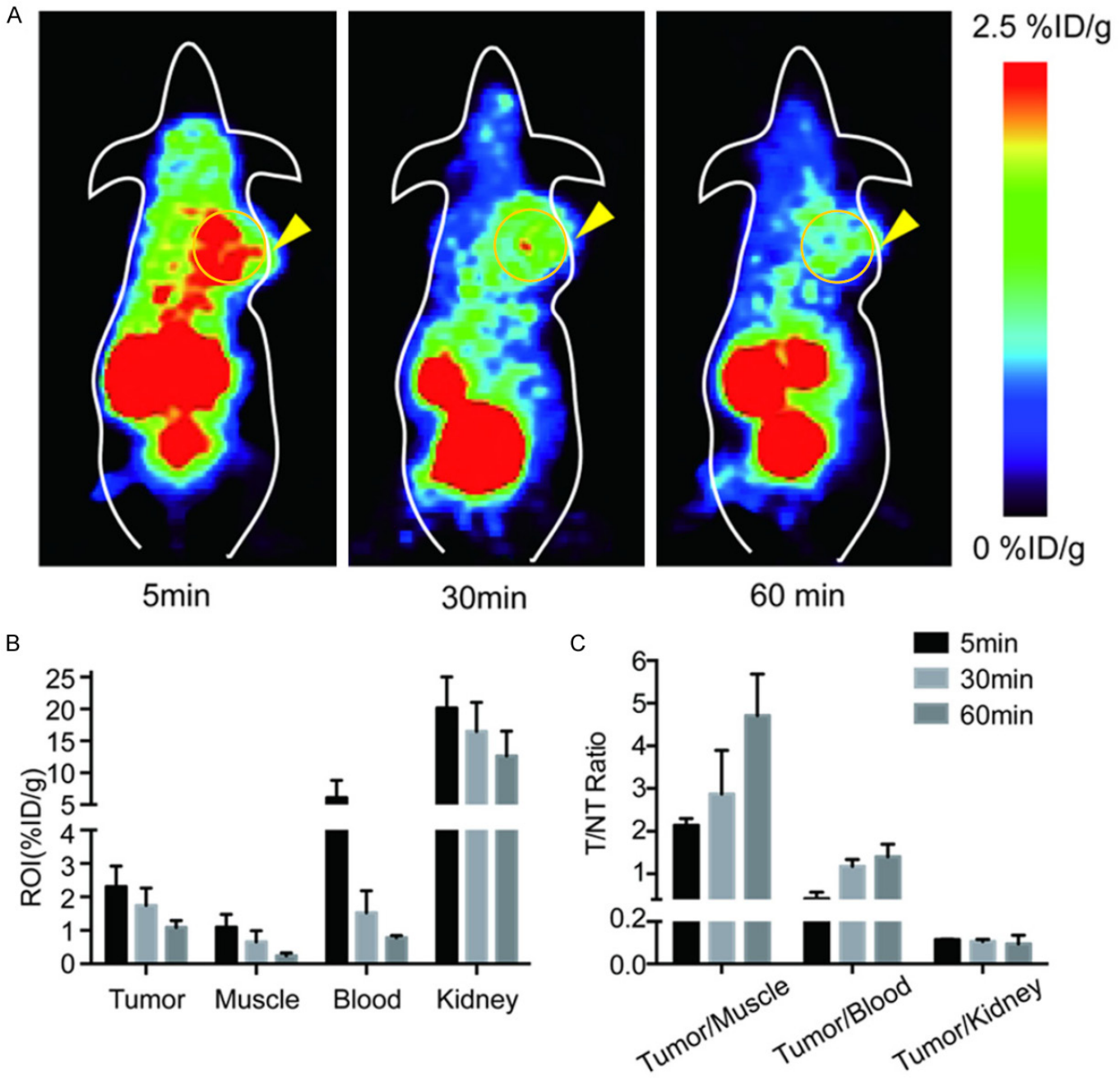

Figure 4. Representative static PET images of ^{68}Ga-DOTA-TMTP1 in Hela tumor xenografts at different time points. A. Whole-body coronal PET images of Hela tumor-bearing mice at 5, 30 and 60 min after injection of 7.4 MBq (200 μCi) of ^{68}Ga-DOTA-TMTP1. Yellow arrows indicate tumor regions. B. The quantitative uptake of tumor by plotting ROI in Hela tumor, muscle, blood and kidney. C. Tumor to muscle, blood and kidney ratios of ^{68}Ga-DOTA-TMTP1 in tumor-bearing mice. Data are expressed as mean ± SD.

reached a peak at 40 s post injection in the kidneys (28.87 ± 6.34 %ID/g) and then decreased to 5.20 ± 1.10 %ID/g at 60 min. ^{68}Ga-DOTA-TMTP1 showed rapid blood clearance (8.30 ± 0.81 %ID/g at 1 s after injection, 1.77 ± 0.15 %ID/g at 10 min, and 0.25 ± 0.04 %ID/g at 60 min after injection). The uptake in muscles gradually increased in 60 s (1.03 ± 0.35 %ID/g at 1 min) and remained relatively stable within 10 min (0.83 ± 0.38 %ID/g at 10 min), and then gradually decreased to 0.16 ± 0.11 %ID/g at 60 min post injection.

Representative static microPET images at 5, 30, 60 min after intravenous injection of ^{68}Ga-DOTA-TMTP1 (about 200 μCi) are shown in **Figure 4A**. Tumor and major organ activity accumulation was quantified by measuring the ROIs that enclosed the entire organ on the coronal images. The kinetics of the tracer in the tumor, muscle, blood, and kidneys are shown in **Figure 4B**. The tumors were clearly visible with high contrast in relation to the contralateral background at 30 and 60 min time points. The tumor uptake of ^{68}Ga-DOTA-TMTP1 was determined to be 2.31 ± 0.61 %ID/g, 1.75 ± 0.52 %ID/g and 1.09 ± 0.20 %ID/g at 5, 30, and 60 min (**Figure 4B**). Prominent uptake of ^{68}Ga-DOTA-TMTP1 was observed in the kidneys and bladder suggesting that this tracer is mainly excreted through the renal-urinary route. After clearance of the

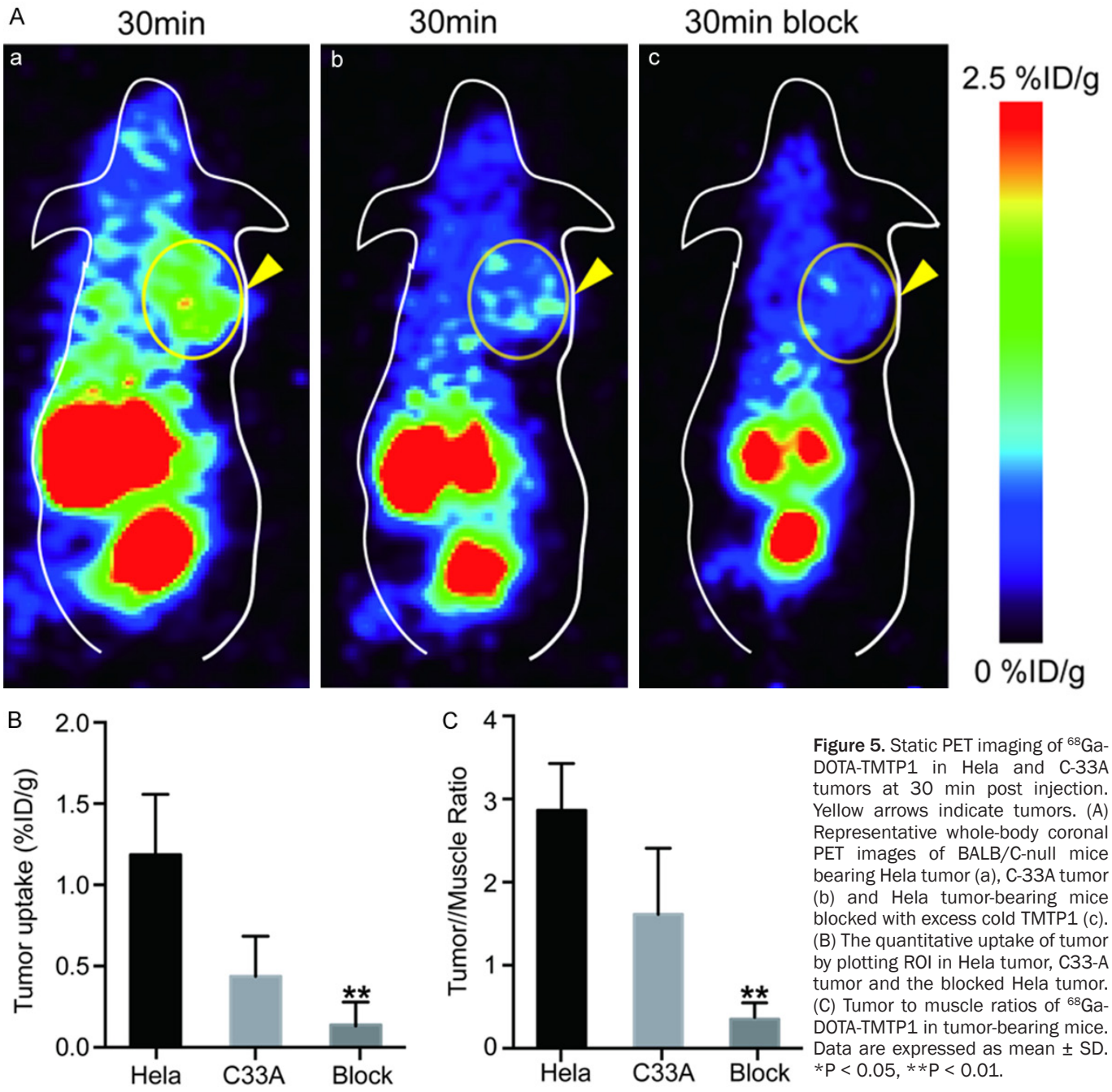

Figure 5. Static PET imaging of ^{68}Ga-DOTA-TMTP1 in Hela and C-33A tumors at 30 min post injection. Yellow arrows indicate tumors. (A) Representative whole-body coronal PET images of BALB/C-null mice bearing Hela tumor (a), C-33A tumor (b) and Hela tumor-bearing mice blocked with excess cold TMTP1 (c). (B) The quantitative uptake of tumor by plotting ROI in Hela tumor, C33-A tumor and the blocked Hela tumor. (C) Tumor to muscle ratios of ^{68}Ga-DOTA-TMTP1 in tumor-bearing mice. Data are expressed as mean ± SD. *P < 0.05, **P < 0.01.

tracer from the blood and normal organs, the tumor/muscle and tumor/blood ratios increased with time as shown in **Figure 4C**.

According to the cell uptake and efflux assays, Hela showed better affinity for ^{68}Ga-DOTA-TMTP1 than C-33A. Representative static scanning images of Hela and C-33A-tumor bearing mice at 30 min post injection of ^{68}Ga-DOTA-TMTP1 are shown in **Figure 5A**. The uptake of ^{68}Ga-DOTA-TMTP1 in Hela tumor was higher than that in C-33A tumor (**Figure 5B**). Using contralateral muscle as background, tumor-to-muscle ratio in Hela tumor was also higher than that in C-33A tumor (**Figure 5C**).

The in vivo specificity of ^{68}Ga-DOTA-TMTP1 was confirmed by blocking studies. Considering that at the time point of 30 minutes, the tumor was clearly visible with high contrast in relation to the contralateral background, the blocking study was performed in Hela-tumor bearing mice preinjected with excess cold TMTP1 at 30 min prior to injection of ^{68}Ga-DOTA-TMTP1. Representative images of Hela-tumor bearing mice at 30 min after injection of ^{68}Ga-DOTA-TMTP1 in the presence of TMTP1 (15 mg/kg) are shown in **Figure 5A**. The tumor uptake of ^{68}Ga-DOTA-TMTP1 was significantly inhibited by TMTP1 (**Figure 5B**). Tumor-to-muscle ratio was lower in blocked tumor than in unblocked mice (**Figure 5C**).

Biodistribution studies

The biodistribution study of ^{68}Ga-DOTA-TMTP1 was performed in nude mice bearing Hela tumors. Each mouse

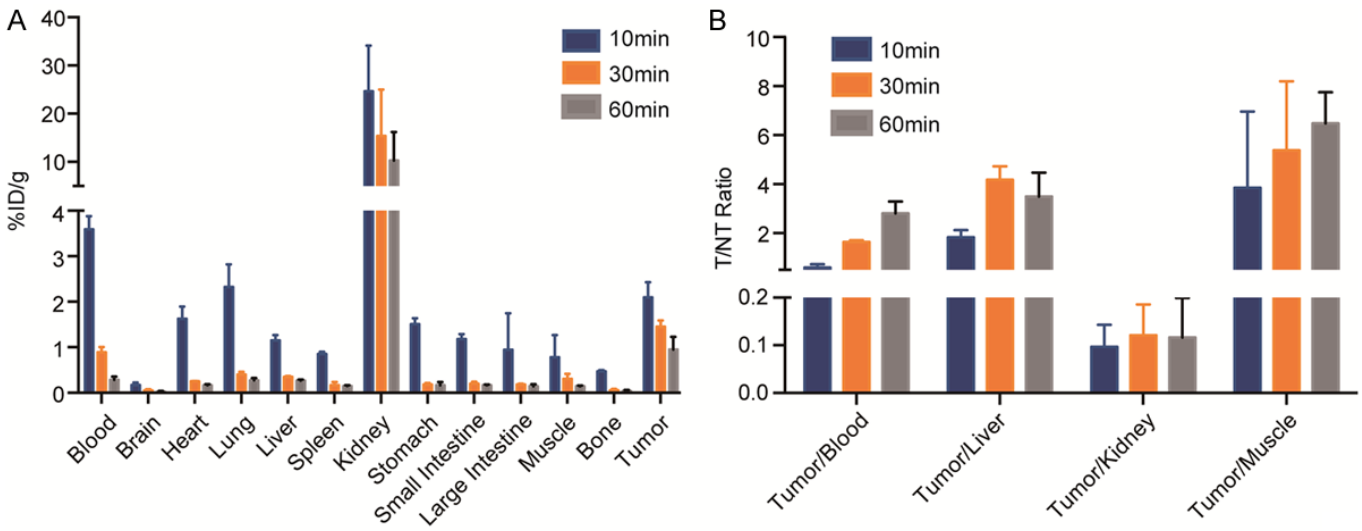

Figure 6. Biodistribution of ^{68}Ga-DOTA-TMTP1 in Hela tumor-bearing mice. (A) Biodistribution and (B) its related tumor-to-normal-tissue (T/NT) ratios of ^{68}Ga-DOTA-TMTP1 in Hela tumor-bearing nude mice at 10, 30, 60 min after intravenous injection. Data are expressed as mean ± SD.

Table 1. Biodistribution and tumor-to-normal-tissue ratios of ^{68}Ga-DOTA-TMTP1 after intravenous injection in Hela cervical cancer bearing athymic mice

Organ	10 min		30 min		60 min	
	%ID/g	T/NT	%ID/g	T/NT	%ID/g	T/NT
Blood	3.59 ± 0.29	0.59 ± 0.14	0.89 ± 0.12	1.64 ± 0.07	0.29 ± 0.07	2.81 ± 0.49
Brain	0.16 ± 0.07	12.63 ± 3.17	0.05 ± 0.03	34.71 ± 17.50	0.03 ± 0.01	38.00 ± 13.94
Heart	1.62 ± 0.27	1.32 ± 0.32	0.25 ± 0.01	5.75 ± 0.65	0.17 ± 0.02	5.63 ± 1.10
Lung	2.32 ± 0.50	0.91 ± 0.08	0.40 ± 0.06	3.69 ± 0.68	0.28 ± 0.05	3.46 ± 0.96
Liver	1.15 ± 0.11	1.83 ± 0.30	0.35 ± 0.02	4.18 ± 0.55	0.27 ± 0.02	3.50 ± 0.97
Spleen	0.85 ± 0.05	2.45 ± 0.31	0.16 ± 0.07	9.84 ± 3.92	0.15 ± 0.02	6.55 ± 2.52
Kidney	24.65 ± 9.45	0.10 ± 0.05	15.38 ± 9.61	0.12 ± 0.06	10.30 ± 5.92	0.12 ± 0.08
Stomach	1.51 ± 0.13	1.39 ± 0.12	0.18 ± 0.03	8.30 ± 1.96	0.17 ± 0.07	6.07 ± 1.33
Small Intestine	1.18 ± 0.11	1.77 ± 0.22	0.20 ± 0.04	7.39 ± 1.21	0.17 ± 0.02	5.78 ± 1.89
Large Intestine	0.95 ± 0.80	3.43 ± 2.15	0.13 ± 0.05	8.05 ± 0.27	0.09 ± 0.01	6.82 ± 2.50
Muscle	0.78 ± 0.49	3.85 ± 3.11	0.20 ± 0.05	5.38 ± 2.82	0.10 ± 0.03	6.48 ± 1.27
Bone	0.47 ± 0.03	4.47 ± 0.78	0.06 ± 0.03	27.29 ± 9.87	0.04 ± 0.02	24.71 ± 10.37
Tumor	2.10 ± 0.33	NA	1.45 ± 0.14	NA	0.95 ± 0.28	NA

Data are mean ± SD.

was injected with 100 μCi of ^{68}Ga-DOTA-TMTP1 and then killed at 10, 30, 60 min after injection. **Figure 6A** and **Table 1** show that the tracer uptake decreased between 10 min to 1 h in the Hela tumors and most of the examined organs. The tumor uptake was 2.10 ± 0.33 %ID/g at 10 min and 0.95 ± 0.28 %ID/g at 60 min. In accordance with the imaging results, radioactivity in kidneys was the highest in our models, further supporting renal-urinary metabolism as the main excretory route. The tracer exhibited rapid blood clearance, with 3.59 ± 0.29, 0.89 ± 0.12, and 0.29 ± 0.07 %ID/g remaining in blood at 10, 30, and 60 min, respectively. The uptake and retention of ^{68}Ga-DOTA-TMTP1 in all the organs except kidney were relatively low at 60 min post-injection. The T/NT ratios of ^{68}Ga-DOTA-TMTP1 are presented in **Figure 6B** and **Table 1**.

Discussion

The metastasis and recurrence of cervical cancer have poor prognoses and early intervention leads to an increased survival rate. Clinical application of ^{18}F-FDG PET/CT has played substantial roles in the diagnosis, treatment response assessment and follow-up of cervical cancer patients [22]. However, ^{18}F-FDG PET/CT shows low efficacy in screening of early-stage cervical cancer and in differentiating cervical cancer from benign tumors or inflammation [3]. For example, high FDG uptake can also be observed in degenerate leiomyomas or early postoperative pelvic tissues [3, 23]. Moreover, ^{18}F-FDG may provide false-negative results in tiny lesions. Therefore, developing novel molecular imaging agents may somehow assist in diagnosis.

Peptides are ideal targeting ligands because of their small size, high affinity, rapid tissue penetration and low immunogenicity [24]. They can be used as vectors for molecular imaging and tumor-targeting therapy. TMTP1 (Asn-Val-Val-Arg-Gln, NVVRQ) is a novel five-amino acid peptide previously identified by our group. TMTP1 specifically binds to highly metastatic cancer cells as well as metastasis foci and even occult metastasis but not towards poorly metastatic or non-metastatic cell lines [7]. Until now, several TMTP1 based radiotracers have been developed for the imaging of highly metastatic cancers by PET or SPECT [12, 25]. PET is one of the rare molecular imaging technologies approved by Food and Drug Association (FDA) [26]. It provides higher spatial resolution and sensitivity than SPECT and plays a key role in cancer staging, restaging and treatment evaluation of cancers as well as various diseases [16, 18, 27]. Instead of ^{18}F or ^{64}Cu, we preferred ^{68}Ga as the positron emitter because of the accessibility of kit formation and does not require use of a cyclotron [16, 28].

In this study, we have designed, synthesized and evaluated a TMTP1-based peptide that was radiolabeled with ^{68}Ga via DOTA chelator to develop a novel tumor imaging tracer. The cyclic TMTP1 peptide was designed by a disulfide bond with two cysteine residues and glycine residues provide spacer function which allow physical formation of a loop structure. This cyclic structure may increase the stability of the tracer and improve uptake by tumors. DOTA is a common commercial chelator that can be used for fast and efficient ^{68}Ga labeling [29]. DOTA was coupled to the peptides via a triglycine (Gly_3) linker which provides a spacer function so that TMTP1 motif can achieve simultaneous binding to tumor cells and radiotracer excretion from normal tissues and organs [30].

Under optimized conditions, ^{68}Ga-DOTA-TMTP1 exhibited a high yield and high radiochemical purity. The radiotracer was stable in both saline and human serum. In vitro studies have shown that ^{68}Ga-DOTA-TMTP1 displayed higher cellular uptake in Hela cells which have high metastatic potential and relatively lower uptake in C-33A tumor cells with low metastatic potential, indicating that ^{68}Ga-DOTA-TMTP1 could provide more sensitive PET imaging in highly metastatic tumor models. ^{68}Ga-DOTA-TMTP1 revealed the lowest affinity to normal cervical cancer cell line End1. XPNPEP2, also known as aminopeptidase P, may be a potential receptor of TMTP1 (unpublished data) and has been found to be overexpressed in cervical cancer [7, 8]. Our group had previously reported that Hela presented higher expression of XPNPEP2 than C-33A while End1 exhibited the lowest [8]. ^{68}Ga-DOTA-TMTP1 might pass through tumor cell membrane via passive infiltration or some possible targeted receptors, such as XPNPEP2. The precise mechanisms need to be further studied. Furthermore, microPET imaging of ^{68}Ga-DOTA-TMTP1 was evaluated in mice carrying Hela and C-33A tumors. Higher uptake of ^{68}Ga-DOTA-TMTP1 was observed in Hela tumor xenografts which may be due to high density of XPNPEP2 expression. The small molecular size of ^{68}Ga-DOTA-TMTP1 and its hydrophilicity results in fast clearance from non-target tissues and blood. Tumor-to-muscle ratio increased with time and Hela tumor could be clearly visualized after injection of the radiotracer. The tumor-to-muscle ratios in microPET were higher than 2.0 at 5 min and increased over time. The specificity of ^{68}Ga-DOTA-TMTP1 in in vitro and in vivo was confirmed by the blocking studies. The tumor uptake of ^{68}Ga-DOTA-TMTP1 can be significantly blocked using an excess of cold TMTP1, indicating that the major fraction of the radiotracer is specific and the tracer mimics the features of TMTP1 to target receptors.

Biodistribution experiments could determine the accumulation of ^{68}Ga-DOTA-TMTP1 in tumor and major organs more accurately and be further verified by microPET imaging studies. Hela tumors showed rapid uptake of ^{68}Ga-DOTA-TMTP1 while most organs presented low level uptake. Most of tumor-to-tissue ratios increased with time, making the tracer a promising agent for highly metastatic tumor imaging. Moreover, the remarkable accumulation of ^{68}Ga-DOTA-TMTP1 in the kidneys which was observed in both microPET and biodistribution studies may due to its hydrophilic nature or its expressing mechanism since XPNPEP2 is also highly expressed in the kidneys when compared to other tissues [31]. Although the high uptake of radiotracers in the kidneys rarely interferes with imaging readings or analysis [32], it is necessary to improve the kinetic properties of the tracer and reduce accumulation in the kidneys. In this study, the ratios of the tumor-to-muscle reached 6.48 and tumor-to-liver exceeded 3.5 which is higher than those of ^{99m}Tc-HYNIC-TMTP1 and [^{18}F]AlF-NOTA-G-TMTP1. The tumor uptake of ^{68}Ga-labeled TMTP1 was higher than that of ^{99m}Tc labeled TMTP1. Since the tumor uptake of ^{68}Ga-DOTA-TMTP1 is not very high when compared to other tracers, further efforts in enhancing the binding affinity of ^{68}Ga-DOTA-TMTP1 can be employed, such as multimerization, mutireceptor-targeting heterodimerization and non-binding site modification [33].

^{18}F-FDG PET/CT is a functional metabolic imaging technique detecting of cellular metabolism, thus it is not truly tumor specific. ^{18}F-FDG PET/CT shows limited efficacy in screening of early-stage cervical cancer and in differentiating cervical cancer from benign tumors or inflammation. TMTP1 specifically binds to highly metastatic cancer cells as well as metastasis foci and even occult metastasis but not towards poorly metastatic or non-metastatic cell lines. In the course of this study, we have designed and preliminarily evaluated ^{68}Ga-labeled TMTP1 as a novel radiotracer for tumor imaging. MicroPET and biodistribution results suggest the likelihood of ^{68}Ga-DOTA-TMTP1 for targeting highly metastatic cervical cancer. Therefore, ^{68}Ga-DOTA-TMTP1 is a promising radiotracer appling in the detection of minimal focus with early stage, differential diagnosis between benign and malignant diseases, and guiding treatment.

Conclusions

This study originally employs ^{68}Ga labeled TMTP1 peptide for PET imaging in cervical cancer models. ^{68}Ga-DOTA-TMTP1 was produced rapidly with high yield and high purity and it was found to be a promising PET tracer for targeting highly metastatic cervical cancer exhibiting excellent stability, high specificity and good pharmacokinetic properties.

Acknowledgements

This work was supported by the grants from National Science Foundation of China (22104040, 82272628, 81601526), and Co-operation Research Plan of Medical Science and Technology of Henan Province (No. LHGJ20220415). The authors thank Dr. Rajluxmee Beejadhursing for revision of the manuscript.

Disclosure of conflict of interest

None.

Address correspondence to: Qingjian Dong, Department of Nuclear Medicine, Tongji Hospital, Tongji Medical College, Huazhong University of Science and Technology, Wuhan 430030, Hubei, China. E-mail: dongqingjian@hust.edu.cn; Can Zhao, Department of Pathology, Tongji Hospital, Tongji Medical College, Huazhong University of Science and Technology, Wuhan 430030, Hubei, China. E-mail: 373583984@qq.com

References

[1] Bray F, Ferlay J, Soerjomataram I, Siegel RL, Torre LA and Jemal A. Global cancer statistics 2018: GLOBOCAN estimates of incidence and mortality worldwide for 36 cancers in 185 countries. CA Cancer J Clin 2018; 68: 394-424.

[2] Arbyn M, Weiderpass E, Bruni L, de Sanjose S, Saraiya M, Ferlay J and Bray F. Estimates of incidence and mortality of cervical cancer in 2018: a worldwide analysis. Lancet Glob Health 2020; 8: e191-e203.

[3] Palaniswamy SS, Borde CR and Subramanyam P. 18F-FDG PET/CT in the evaluation of cancer cervix: where do we stand today? Nucl Med Commun 2018; 39: 583-592.

[4] Benedet JL, Bender H, Jones H 3rd, Ngan HY and Pecorelli S. FIGO staging classifications and clinical practice guidelines in the management of gynecologic cancers. FIGO Committee on Gynecologic Oncology. Int J Gynaecol Obstet 2000; 70: 209-262.

[5] Waggoner SE. Cervical cancer. Lancet 2003; 361: 2217-2225.

[6] Sakurai H, Suzuki Y, Nonaka T, Ishikawa H, Shioya M, Kiyohara H, Katoh H, Nakayama Y, Hasegawa M and Nakano T. FDG-PET in the detection of recurrence of uterine cervical carcinoma following radiation therapy--tumor volume and FDG uptake value. Gynecol Oncol 2006; 100: 601-607.

[7] Yang W, Luo D, Wang S, Wang R, Chen R, Liu Y, Zhu T, Ma X, Liu R, Xu G, Meng L, Lu Y, Zhou J and Ma D. TMTP1, a novel tumor-homing peptide specifically targeting metastasis. Clin Cancer Res 2008; 14: 5494-5502.

[8] Cheng T, Wei R, Jiang G, Zhou Y, Lv M, Dai Y, Yuan Y, Luo D, Ma D, Li F and Xi L. XPNPEP2 is overexpressed in cervical cancer and promotes cervical cancer metastasis. Tumour Biol 2017; 39: 1010428317717122.

[9] Liu R, Xi L, Luo D, Ma X, Yang W, Xi Y, Wang H, Qian M, Fan L, Xia X, Li K, Wang D, Zhou J, Meng L, Wang S and Ma D. Enhanced targeted anticancer effects and inhibition of tumor metastasis by the TMTP1 compound peptide TMTP1-TAT-NBD. J Control Release 2012; 161: 893-902.

[10] Ma X, Xi L, Luo D, Liu R, Li S, Liu Y, Fan L, Ye S, Yang W, Yang S, Meng L, Zhou J, Wang S and Ma D. Anti-tumor effects of the peptide TMTP1-GG-D(KLAKLAK)(2) on highly metastatic cancers. PLoS One 2012; 7: e42685.

[11] Liu R, Ma X, Wang H, Xi Y, Qian M, Yang W, Luo D, Fan L, Xia X, Zhou J, Meng L, Wang S, Ma D and Xi L. The novel fusion protein sTRAIL-TMTP1 exhibits a targeted inhibition of primary tumors and metastases. J Mol Med (Berl) 2014; 92: 165-175.

[12] Li F, Cheng T, Dong Q, Wei R, Zhang Z, Luo D, Ma X, Wang S, Gao Q, Ma D, Zhu X and Xi L. Evaluation of (99m)Tc-HYNIC-TMTP1 as a tumor-homing imaging agent targeting metastasis with SPECT. Nucl Med Biol 2015; 42: 256-262.

[13] Ma X, Lv P, Ye S, Zhang Y, Li S, Kan C, Fan L, Liu R, Luo D, Wang A, Yang W, Yang S, Bai X, Lu Y, Ma D, Xi L and Wang S. DT390-triTMTP1, a novel fusion protein of diphtheria toxin with tandem repeat TMTP1 peptide, preferentially targets metastatic tumors. Mol Pharm 2013; 10: 115-126.

[14] Li Y, Zhang D, Shi Y, Guo Z, Wu X, Ren JL, Zhang X and Wu H. Syntheses and preliminary evaluation of [(18)F]AlF-NOTA-G-TMTP1 for PET imaging of high aggressive hepatocellular carcinoma. Contrast Media Mol Imaging 2016; 11: 262-271.

[15] Knetsch PA, Petrik M, Griessinger CM, Rangger C, Fani M, Kesenheimer C, von Guggenberg E, Pichler BJ, Virgolini I, Decristoforo C and Haubner R. [68Ga]NODAGA-RGD for imaging alphavbeta3 integrin expression. Eur J Nucl Med Mol Imaging 2011; 38: 1303-1312.

[16] Tolmachev V and Orlova A. Influence of labelling methods on biodistribution and imaging properties of radiolabelled peptides for visualisation of molecular therapeutic targets. Curr Med Chem 2010; 17: 2636-2655.

[17] Al-Nahhas A, Win Z, Szyszko T, Singh A, Khan S and Rubello D. What can gallium-68 PET add to receptor and molecular imaging? Eur J Nucl Med Mol Imaging 2007; 34: 1897-1901.

[18] Martiniova L, Palatis L, Etchebehere E and Ravizzini G. Gallium-68 in medical imaging. Curr Radiopharm 2016; 9: 187-207.

[19] Liu Z, Niu G, Wang F and Chen X. (68)Ga-labeled NOTA-RGD-BBN peptide for dual integrin and GRPR-targeted tumor imaging. Eur J Nucl Med Mol Imaging 2009; 36: 1483-1494.

[20] Kido A and Nakamoto Y. Implications of the new FIGO staging and the role of imaging in cervical cancer. Br J Radiol 2021; 94: 20201342.

[21] Atri M, Zhang Z, Dehdashti F, Lee SI, Ali S, Marques H, Koh WJ, Moore K, Landrum L, Kim JW, DiSilvestro P, Eisenhauer E, Schnell F and Gold M. Utility of PET-CT to evaluate retroperitoneal lymph node metastasis in advanced cervical cancer: results of ACRIN6671/GOG0233 trial. Gynecol Oncol 2016; 142: 413-419.

[22] Rao YJ and Grigsby PW. The role of PET imaging in gynecologic radiation oncology. PET Clin 2018; 13: 225-237.
[23] Kitajima K, Murakami K, Yamasaki E, Kaji Y and Sugimura K. Standardized uptake values of uterine leiomyoma with 18F-FDG PET/CT: variation with age, size, degeneration, and contrast enhancement on MRI. Ann Nucl Med 2008; 22: 505-512.
[24] Benedetti E, Morelli G, Accardo A, Mansi R, Tesauro D and Aloj L. Criteria for the design and biological characterization of radiolabeled peptide-based pharmaceuticals. BioDrugs 2004; 18: 279-295.
[25] Yao L, Wen X, Guo W, Fang J, Zhang X, Guo Z, Huang J and Li Y. Novel radiolabeled TMTP1 for long-acting hepatocellular carcinoma therapeutics. Mol Pharm 2022; 19: 3178-3186.
[26] Juweid ME and Cheson BD. Positron-emission tomography and assessment of cancer therapy. N Engl J Med 2006; 354: 496-507.
[27] Gambhir SS. Molecular imaging of cancer with positron emission tomography. Nat Rev Cancer 2002; 2: 683-693.
[28] Meyer GJ, Macke H, Schuhmacher J, Knapp WH and Hofmann M. 68Ga-labelled DOTA-derivatised peptide ligands. Eur J Nucl Med Mol Imaging 2004; 31: 1097-1104.
[29] Notni J, Pohle K and Wester HJ. Comparative gallium-68 labeling of TRAP-, NOTA-, and DOTA-peptides: practical consequences for the future of gallium-68-PET. EJNMMI Res 2012; 2: 28.
[30] Shi J, Wang L, Kim YS, Zhai S, Liu Z, Chen X and Liu S. Improving tumor uptake and excretion kinetics of 99mTc-labeled cyclic arginine-glycine-aspartic (RGD) dimers with triglycine linkers. J Med Chem 2008; 51: 7980-7990.
[31] Ersahin C, Szpaderska AM, Orawski AT and Simmons WH. Aminopeptidase P isozyme expression in human tissues and peripheral blood mononuclear cell fractions. Arch Biochem Biophys 2005; 435: 303-310.
[32] Jeong JM, Hong MK, Chang YS, Lee YS, Kim YJ, Cheon GJ, Lee DS, Chung JK and Lee MC. Preparation of a promising angiogenesis PET imaging agent: 68Ga-labeled c(RGDyK)-isothiocyanatobenzyl-1,4,7-triazacyclononane-1,4,7-triacetic acid and feasibility studies in mice. J Nucl Med 2008; 49: 830-836.
[33] Zhao M, Yang W, Zhang M, Li G, Wang S, Wang Z, Ma X, Kang F and Wang J. Evaluation of (68)Ga-labeled iNGR peptide with tumor-penetrating motif for microPET imaging of CD13-positive tumor xenografts. Tumour Biol 2016; 37: 12123-12131.

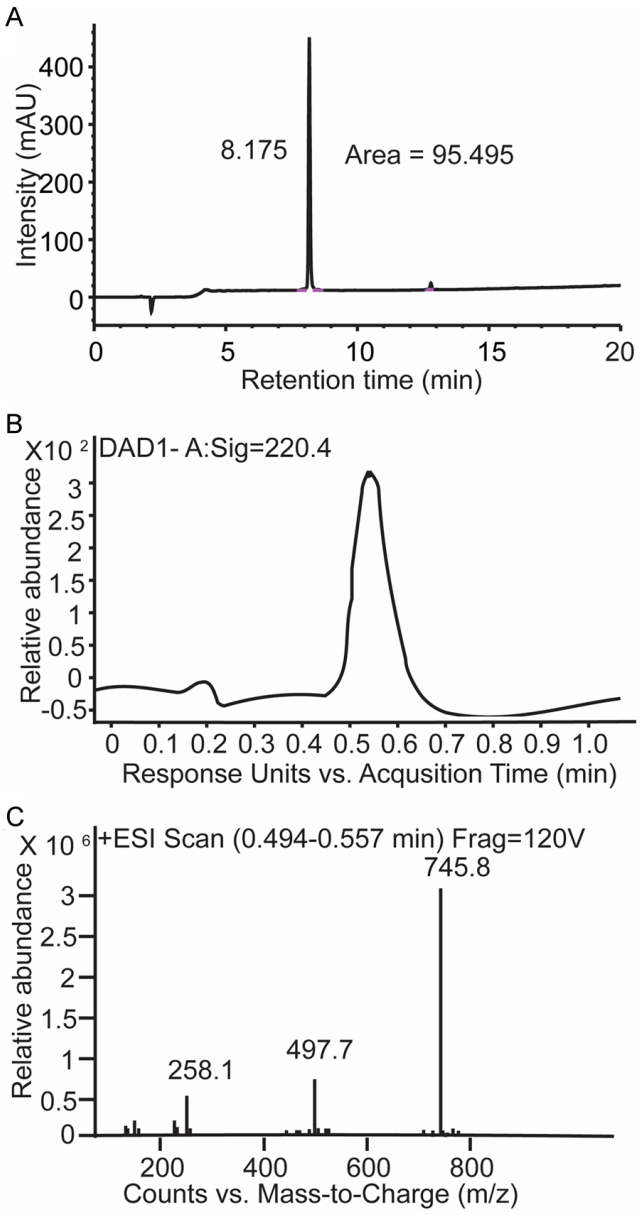

Supplementary Figure 1. Quality test of DOTA-TMTP1. A. HPLC chromatogram of DOTA-TMTP1. The retention time is 8.175 min and the purity of this compound reaches 95.495%. B and C. The LC-MS (ESI scan) confirms the correct synthesis of DOTA-TMTP1.